

Shear stress relaxation in liquids

Janka Petracic

Citation: *The Journal of Chemical Physics* **120**, 10188 (2004); doi: 10.1063/1.1735628

View online: <http://dx.doi.org/10.1063/1.1735628>

View Table of Contents: <http://scitation.aip.org/content/aip/journal/jcp/120/21?ver=pdfcov>

Published by the [AIP Publishing](#)

Articles you may be interested in

[The origin of persistent shear stress in supercooled liquids](#)

J. Chem. Phys. **137**, 014506 (2012); 10.1063/1.4730912

[Mechanism of stress relaxation in Ge nanocrystals embedded in Si O 2](#)

Appl. Phys. Lett. **86**, 063107 (2005); 10.1063/1.1856132

[Stress Relaxation of a Branched Polybutadiene in Double-Step Shear Deformations](#)

J. Rheol. **29**, 533 (1985); 10.1122/1.549801

[Stress Relaxation and Differential Dynamic Modulus of Polyisobutylene in Large Shearing Deformations](#)

J. Rheol. **29**, 273 (1985); 10.1122/1.549791

[Relaxation of Shear and Normal Stresses in Double-Step Shear Deformations for a Polystyrene Solution. A Test of the Doi-Edwards Theory for Polymer Rheology](#)

J. Rheol. **25**, 549 (1981); 10.1122/1.549650



AIP | APL Photonics

APL Photonics is pleased to announce
Benjamin Eggleton as its Editor-in-Chief



Shear stress relaxation in liquids

Janka Petravica^{a)}

Research School of Chemistry, The Australian National University, Canberra ACT 0200, Australia

(Received 12 December 2003; accepted 9 March 2004)

We show that at high densities, as the system size decreases, liquid becomes able to permanently sustain increasing internal shear stress after a constant deformation, although the other characteristic liquid properties, such as the pair distribution function and diffusion coefficient do not change under strain. The system size necessary for observation of this effect increases with the decrease in temperature, and it is stronger in pair potentials with steeper repulsive part. We relate this result to the size of the “cooperatively rearranging regions” of the Adam–Gibbs theory of glass transition.

© 2004 American Institute of Physics. [DOI: 10.1063/1.1735628]

I. INTRODUCTION

Solids behave elastically under small deformations: they store the deformation energy and sustain shear stress proportional to strain. This ability is the consequence of the vanishing diffusion resulting in the impossibility of further rearrangement of atoms, i.e., motion other than oscillatory around the shifted (“strained”) lattice sites. The crystal shear modulus is therefore primarily a potential energy modulus.¹

A liquid can store deformation energy and sustain shear stress only for a time shorter than its shear stress relaxation time, before all energy is dissipated to the environment and all shear stress relaxes. The mechanism of decay of shear modulus is in the nonvanishing liquid diffusion coefficient, which makes possible the complete particle rearrangement in a flow with viscous dissipation of heat. The relaxation time is the average time needed for rearrangement into a configuration without shear stress. The liquid does not lose its high-frequency shear rigidity, but since atomic rearrangements become possible, the modulus ceases to be simply described in potential energy terms and takes on an entropic character.¹

Atomic rearrangement that is at the bottom of the relaxation process occurs not only during time, but also over space. This idea is the basis of the Adam–Gibbs theory of glass transition.² In order that shear stress can relax in time, it must be possible to have a configuration that incorporates the boundary strain irreversibly into the structure of the material in such a way that the stresses disappear while the strains remain. As the system is rearranged into this configuration, the shear modulus gradually falls to zero. However, at high density and low temperature, the number of possible configurations in a small subsystem with prescribed boundary conditions becomes scarce. One needs progressively larger groupings of atoms in order to obtain configurations without stress irrespective of the conditions at the boundaries. This leads to the definition of a “cooperatively rearranging region” as a group of atoms that can rearrange itself into different configurations independent of its environment. As the liquid is cooled, cooperatively rearranging regions

grow and relaxations require coordinated participation of a larger number of atoms, thus increasing the relaxation time. The Adam–Gibbs theory relates the growth in relaxation time to the decrease in configurational entropy associated with supercooling on account of the growth of cooperatively rearranging regions.

The size of the region thus provides a definition for a divergent length scale which would accompany the glass transition. However, the theory does not say anything about the nature of this region and provides no prescription about calculating its size. Since the appearance of the Adam–Gibbs theory, there has been a search for a plausible physical entity that could represent the “cooperatively rearranging region.” In most work they were speculated to be “domains” of distinct order (e.g., icosahedral clusters or “amorphons”³) separated by distinct “domain walls” and characterized by slower (arrested) dynamics compared to the rest of the system. The search for these objects in experiments and molecular simulations gave contradictory results.^{3–5}

Later, Mountain⁶ pointed out that the existence of structurally distinct domains is not necessary in order to define a growing length scale in supercooled liquids. He examined the dispersion relation for the transverse momentum current. In solids, a finite shear modulus at zero frequency exists because long wavelength transverse elastic waves can propagate for a long time without damping. In a liquid, long wavelengths are damped fast, but waves of sufficiently short wavelengths and high frequencies can propagate for considerable distances before decaying. Even simple monatomic liquids can therefore support propagating elastic transverse modes with atomic-scale wavelengths. From the dispersion relation, it is possible to estimate the largest wavelength for the transverse mode that a liquid can support. This wavelength increases with the decrease in temperature and measures the size of cooperatively rearranging regions, existing not only in supercooled liquids, but also at elevated temperatures.

The implication in all the above work is that in liquids there is a well-defined correlation length of configurational origin, over which shear stress can relax. This correlation length decreases with the increase in temperature and is responsible for the change in relaxation time. The direct con-

^{a)}Present address: School of Chemistry F11, The University of Sydney, NSW 2006, Australia. Electronic mail: janka@chem.usyd.edu.au

sequence of this image is that in a liquid system of the size smaller than the size of the cooperatively rearranging region, under strain, shear stress does not relax. We test this idea by performing molecular dynamics simulations of successively smaller liquid systems with strain imposed by periodic boundary conditions.

II. SIMULATION METHOD

The system studied consists of $N=256$ atoms interacting with the Lennard–Jones (LJ) pair potential,

$$\Phi_{ij}(r_{ij}) = 4\phi[(\sigma/r_{ij})^{12} - (\sigma/r_{ij})^6], \quad (1)$$

where r_{ij} is the distance between the particles i and j , σ is the exclusion diameter, and ϕ is the depth of the potential well. In this article we use the LJ reduced system of units, where σ is the unit of distance, ϕ is the unit of energy, and mass is measured in units of particle mass. The potential cutoff was applied at the distance of 2.5σ . This interaction gives rise to the phase diagram containing three phases and their coexistence.⁷

In all cases, the density of the system was $\rho=1.0$. Depending on temperature, at this density the system exists in the liquid and in the solid phase. We studied the influence of strain on the liquid properties for several temperatures above and below the freezing temperature of $T_F=1.46$.⁸

In order to avoid confinement effects, the simulation was done in periodic boundary conditions, which in equilibrium consist of periodic replicas of the simulation cell.⁹ The strained system was represented by periodic cells shifted by a distance Δ in the x direction. The dimensionless strain ε is the ratio of the shift Δ with respect to the sidelength L of the simulation cell, $\varepsilon = \Delta/L$.

The “shifted” periodic boundary conditions (or a static version of the Lees–Edwards “sliding brick” periodic boundaries¹⁰) are identical to a tiling with tilted cells. The geometric equivalence and interchangeability of the two representations is an essential ingredient used in the computer simulation algorithm for constant homogeneous shear flow¹¹ and in the formulation of the Ewald sum for sheared systems with electrostatic interactions.¹²

It is not possible to change instantaneously from an equilibrium simulation cell configuration to a strained configuration because of the atom overlap, so we shear the system at a homogeneous chosen strain rate γ using the so-called Sllod algorithm,¹¹ until the desired deformation is achieved. The equations of motion for the positions \mathbf{r}_i and momenta \mathbf{p}_i ($i=1,\dots,N$) in the equilibrium and the final strained state are

$$\dot{\mathbf{r}}_i = \mathbf{p}_i/m, \quad \dot{\mathbf{p}}_i = \mathbf{F}_i - \alpha \mathbf{p}_i, \quad (2)$$

where \mathbf{F}_i is the total force on the particle i arising from the potential [Eq. (1)]. During shearing the Sllod equations are

$$\dot{\mathbf{r}}_i = \mathbf{p}_i/m + \mathbf{e}_x \gamma r_{yi}, \quad \dot{\mathbf{p}}_i = \mathbf{F}_i - \mathbf{e}_x \gamma p_{yi} - \alpha \mathbf{p}_i, \quad (3)$$

where \mathbf{e}_x is the unit vector in the x direction and γ the strain rate.

Shear causes viscous heating, and we would like the initial and final state to be at the same temperature. Therefore, we add a Gauss thermostat term α to the equations of

motion that fixes the kinetic energy of the system to a constant before, during, and after shear. In the equilibrium and the final strained case it is

$$\alpha = \frac{\sum_{j=1,N} \mathbf{p}_j \cdot \mathbf{F}_j}{\sum_{j=1,N} \mathbf{p}_j^2}, \quad (4)$$

and with the Sllod equations it is equal to

$$\alpha = \frac{\sum_{j=1,N} (\mathbf{p}_j \cdot \mathbf{F}_j - \gamma p_{xi} p_{yi})}{\sum_{j=1,N} \mathbf{p}_j^2}. \quad (5)$$

The presence of a thermostat does not qualitatively affect the equilibrium properties, and can change the value of the ensemble averages to the order of $1/N$ with respect to constant energy simulations. It becomes important in the shear flow simulations with strong strain rate.¹³ It would also strongly affect the shear stress relaxation process when shear stops, because it instantly starts to interpret the remnant velocity profile as heat and causes it to decay faster. However, our interest is not in the decay process but in the final relaxed states, all of which contain no net particle flux and are therefore equivalent to equilibrium.

The equations of motion were solved using the fifth order Gear predictor–corrector integrator with the timestep of 0.001 time units. The system was first equilibrated at the desired temperature for 10^7 time steps, after which it was sheared with strain rates ranging from 0.001 to 10 (in order to check for the strain rate dependence of results) until the chosen strain was reached, and finally equilibrated for the additional 10^7 timesteps for shear stress relaxation to take place.

Viscosity was evaluated in equilibrium and strained states from the Green–Kubo integral. The isotropic nature of a liquid permits the use of a more general form¹⁴ of the Green–Kubo expression, where fluctuations in all the elements of the traceless symmetric stress tensor are taken into account

$$\eta = \frac{V}{k_B T} \int_0^\infty \left\langle \sum_{\alpha,\beta=x,y,z} \Pi_{\alpha\beta}(t) \Pi_{\alpha\beta}(0) \right\rangle dt \quad (6)$$

where V is the volume of the simulation box, k_B is the Boltzmann constant, T is the kinetic temperature defined from the equipartition theorem, and $\Pi_{\alpha\beta}$ are the Cartesian elements of the symmetric traceless pressure tensor.

III. RESULTS

A. Temperature dependence

The rather astonishing simulation results for 256 LJ atoms at three temperatures, $T=2.0$ (pure liquid state), $T=1.5$ (liquid very close to freezing), and $T=1.2$ (supercooled liquid) are shown in Fig. 1 for the periodic boundary conditions with no strain, and for $\varepsilon=0.25$ and $\varepsilon=0.375$. Without any strain, the viscosity integral in Eq. (6) converges to a finite value that, as expected, decreases with increase in temperature. However, in the “strained” periodic boundary conditions, even 10 000 time units after straining, so that there was plenty of time for shear stress to relax, viscosity is infinite. Part of the shear stress never relaxes. The shear

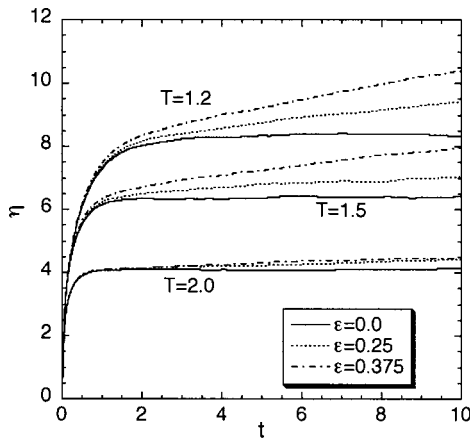


FIG. 1. Viscosity calculated from Eq. (6) for 256 Lennard–Jones atoms at three temperatures and three values of constant strain. The divergence of viscosity in the “strained” periodic boundary conditions disappears at higher temperatures.

stress autocorrelation function does not converge to zero but to finite positive values dependent on strain and decreasing with increase in temperature. Unrelaxed stress definitely still exists above freezing.

The unrelaxed stress is distributed between Π_{xy} and the normal stress differences where the effect is larger (Fig. 2). Notice that Π_{xy} is antisymmetric with respect to strain of 0.5, whereas the diagonal elements of the traceless stress tensor are symmetric. The reason is that at each instant we can regard our simulation cell as a “primitive cell” of a different strained crystal. First, we note that the “lattice” with the strain of $+\varepsilon$ is a mirror image (with respect to the yz plane) of a lattice with the strain $-\varepsilon$. If a configuration is consistent with the strain ε , its mirror image is consistent with $-\varepsilon$. A configuration and its mirror image have the same diagonal elements and Π_{xy} of opposite sign. Next, we observe that the strain of $+\varepsilon$ is identical to the strain of $-(1-\varepsilon)$. Therefore, the strain of $\varepsilon=0.5-\delta$ is the mirror image of $\varepsilon=0.5+\delta$. The strain of 0.5 is a mirror image of -0.5 , so that a configuration and its mirror image are equally probable at $\varepsilon=0.5$, just as for $\varepsilon=0$, and Π_{xy} vanishes on average. Incidentally, normal stresses also vanish for this strain. However,

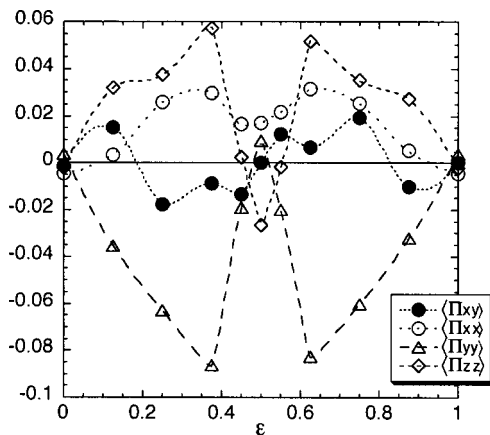


FIG. 2. Strain dependence of average values of the elements of the traceless symmetric stress tensor for the $N=256$ Lennard–Jones system at $T=1.5$.

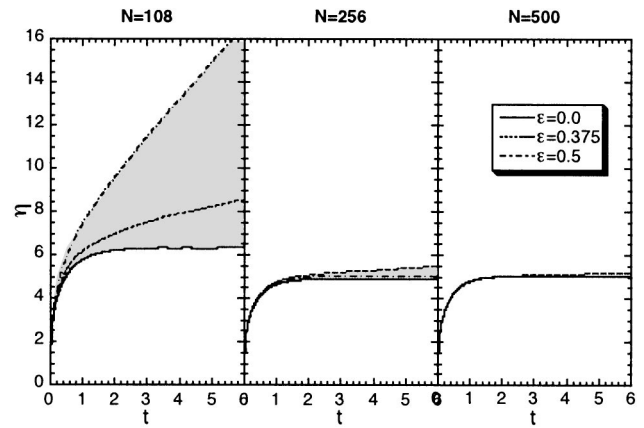


FIG. 3. System size dependence of divergence of viscosity calculated from Eq. (6) for the strained WCA fluid at $T=1.2$.

the fluctuations in Π_{xy} , as it randomly switches from configurations consistent with $\varepsilon=0.5$ and $\varepsilon=-0.5$, are larger than with $\varepsilon=0$ and for this reason viscosity, although not divergent, is higher in the strained system. The difference in viscosities decreases with the increasing temperature.

This result is reproducible in every detail in the sense that it does not at all depend on the manner in which the strained periodic boundary conditions were generated. Exactly the same distribution of stress tensor elements under strain as in Fig. 2 was obtained after relaxation from configurations created with the whole range of strain rates, and with configurations strained and “equilibrated” at the high temperature of 2.5, quenched after equilibration to the temperatures of 1.5 and 1.2 and again equilibrated afterwards.

B. System-size dependence

In order to test the system-size dependence of this effect, we changed from the LJ potential to Weeks–Chandler–Andersen (WCA) potential,¹⁵ which is a shorter-range version with the cutoff at the potential energy minimum (i.e., at the distance of $2^{1/6}\sigma$) and shifted by ϕ , because at this density the Lennard–Jones cutoff left the simulation box. The size-dependence simulations were done at $T=1.2$, where the effects are the strongest.

Decreasing the system size had a huge impact. As shown in Fig. 3, the divergence of viscosity under strain is very fast with $N=108$ while it almost disappears for $N=500$ at the same temperature. The values of the tail of the shear stress autocorrelation function for different strains are shown in Fig. 4. The total average unrelaxed stress decreases rapidly with the increase in the system size. The tail is always positive (shear stress does not reverse its sign) and symmetric with respect to strain of 0.5. For different system sizes the value of the tail has different strain dependence. In the smallest system the largest stress is for the strain of 0.5, and in this case it is purely in the diagonal elements (normal stress differences) for symmetry reasons. As system size is increased, this stress disappears first, and we only see a small increase in viscosity due to increased fluctuations in Π_{xy} .

One would expect the huge unrelaxed stress for the strain of 0.5 in the $N=108$ system to be related to a large difference in structure and potential energy. In fact, the form of the pair distribution function is in both cases (strained and

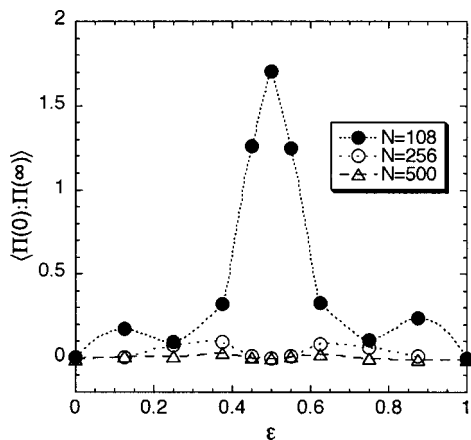


FIG. 4. Strain dependence of the tail of the shear stress autocorrelation function for three sizes of the WCA fluid at $T=1.2$.

unstrained) completely liquidlike, with smooth equidistant peaks showing no peak-splitting structure associated with clustering or crystallization. It is exactly the same in two systems for distances up to half the box length, with only small discrepancies in the corners of the simulation box (Fig. 5). This small difference is responsible for minute variations in potential energy and hydrostatic pressure with strain less than 2% at most with $N=108$.

A change in viscosity is usually closely related to a change in diffusion coefficient (the Stokes–Einstein relationship). Shear stress relaxation is through flow, and large (or infinite) relaxation time intuitively implies low particle mobility and a low diffusion coefficient. One would therefore anticipate a reduced mean square displacement in the strained system, associated with its diverging viscosity. On the contrary, the diffusion coefficient does not change at all with strain, even when the divergence of viscosity is the most dramatic as in the $N=108$ system with $\epsilon=0.5$ (Fig. 6). This result indicates a relationship between diffusion and configurational entropy.^{2,16} There is only one possible configuration (“inherent structure”) corresponding to a strained crystal, therefore there is no diffusion. In a small liquid sys-

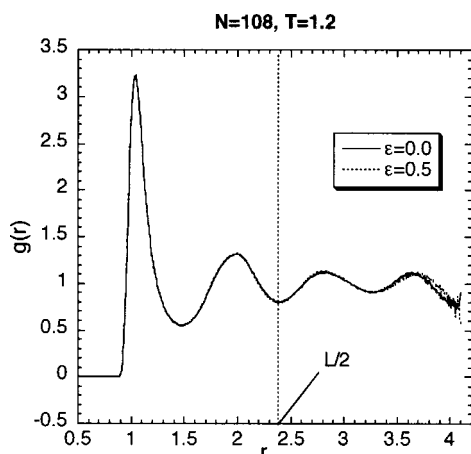


FIG. 5. Pair distribution functions of the equilibrium and strained ($\epsilon=0.5$) WCA fluid at $T=1.2$ up to the corners of the simulation box. The vertical dotted line represents half the box length.

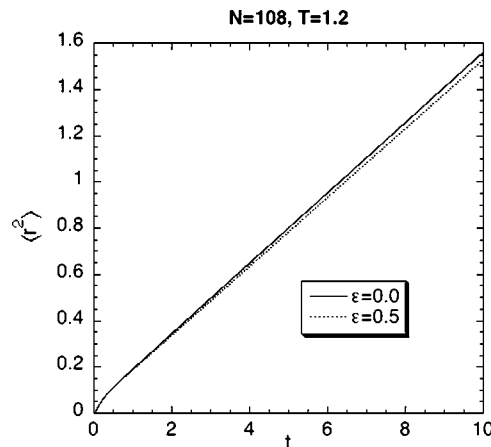


FIG. 6. Mean square displacement for the equilibrium and strained ($\epsilon=0.5$) WCA fluid at $T=1.2$.

tem, there is the same overall number of possible configurations consistent with ordinary and strained boundary conditions, and diffusion does not change. However, the configurations in the strained system are such that they on average contain some shear stress, while the ones in the equilibrium system do not. Again, in accord with the configurational entropy dependence, the diffusion coefficient increases with the system size.

In our simulation this effect is a consequence of the periodic boundary conditions reflected in the minimum image convention, i.e., it is a consequence of the requirement that the density of atoms at \mathbf{r} is the same as at $\mathbf{r} + \epsilon \mathbf{L}_i + \mathbf{L}_j$. In a small dense system this can be achieved only with atomic arrangements that generate shear stress. This is a consequence of the fact that in a small dense system with a given configuration at the surface there are not many possibilities for packing the remaining particles in the volume inside the boundaries. If the boundary conditions contain strain, the majority of arrangements without shear stress are energetically unfavorable, i.e., contain too much particle overlap. In other words, as a consequence of the decrease in configurational entropy (i.e., the number of energetically acceptable configurations) in a small dense system, the nature of the possible packings and the amount of shear stress contained in the system are determined by the configuration at the boundary. In the language of Goldstein,¹ the configurations that “incorporate the boundary strain in such a way that the stresses disappear while the strains remain” are scarce compared to the configurations that incorporate the strained boundary conditions while retaining some unrelaxed shear stress.

Although the simulations of liquid samples with the periodic boundary conditions of any kind are artificial (such systems do not exist in nature), they allow us to study how imposing different boundary conditions on a small subsystem affects its properties. Therefore our result has a physical meaning for bulk liquid systems. In any sufficiently small subsystem with different conditions at boundaries, shear stress will be such as dictated by the boundary conditions and will be correlated over its characteristic length at any instant, although the time average of the shear stress in the subsystem will vanish.

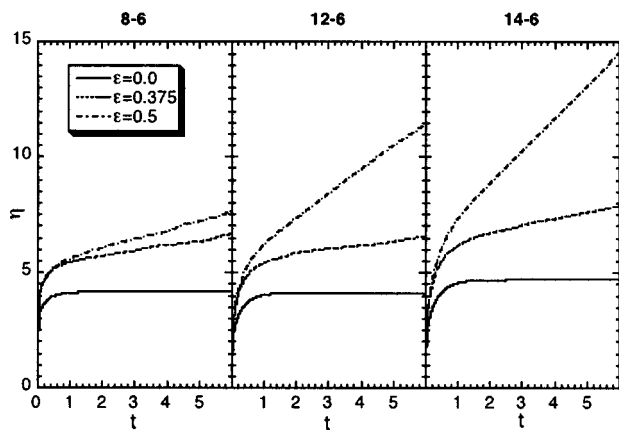


FIG. 7. Divergence of viscosity calculated from Eq. (6) for the strained potentials of different “hardness” at $T = 1.2$.

C. Dependence on potential

Since the unrelaxed stress decreases with the increase in temperature, and the overall consequence of raising the temperature is the increased “softness” of the interaction potential, we compare the effect for the WCA potential and two other short-ranged potentials of different softness, but the same definition of the length and energy scales, σ and ϕ , respectively. The “harder” potential is 14-6 repulsive–attractive:

$$\Phi_{ij}(r_{ij}) = (7/3)^{3/4}(7/4)\phi[(\sigma/r_{ij})^{1/4} - (\sigma/r_{ij})^6] + \phi \quad (7)$$

and the “softer” one is 8–6 repulsive–attractive:

$$\Phi_{ij}(r_{ij}) = 3(4/3)^4\phi[(\sigma/r_{ij})^8 - (\sigma/r_{ij})^6] + \phi. \quad (8)$$

Both have the cutoff at their potential minima, $(7/3)^{1/8}\sigma$ and $(4/3)^{1/2}\sigma$, respectively.

Figure 7 shows the integral of the stress autocorrelation function in Eq. (6) for the three potentials. The divergence of viscosity and the unrelaxed shear stress is by far the largest for the “hardest” potential. This is intuitively acceptable, since if the atoms are soft enough, a sufficient kinetic energy fluctuation permits them to “squeeze” past each other and allows local rearrangements, whereas if they are hard they can rearrange only globally in a cooperative way.

At the same state point with the same system size and under the same strain, the effect is somewhat stronger in a Lennard–Jones than in a WCA system, showing that the long-range cohesive forces increase the cooperative effects. In contrast, a molten sodium chloride system of 216 ions interacting with the Born–Huggins–Meyer potential¹⁷ at the density of 1.7 g/cm³ and at the temperature of 1200 K shows no strain dependence of viscosity, despite the infinite potential range when calculations are done using the Ewald summation. However, it is difficult to draw general conclusions about the influence of the potential range from the properties of the sodium chloride melt for several reasons: there are strong screening effects, the “softness” of the potential depends on pair charges, and only one melting point on the liquid–solid phase diagram is known.¹⁸

IV. CONCLUSION

A small dense liquid system in periodic boundary conditions subjected to constant strain retains liquid structure and diffusion coefficient, but as in a solid its shear stress does not relax. Unrelaxed stress is larger for smaller systems. System size needed for complete stress relaxation under strain decreases with temperature increase. Just like in anomalous crystallization of small systems in periodic boundary conditions,¹⁹ the origin of this effect is purely configurational, a consequence of the scarcity of possible configurations in a small dense system with some constraint on the boundary conditions. In a small subsystem the only configurations that can connect between strained distributions of atoms on the boundaries are those that on average contain some shear stress of configurational origin. In this sense, the critical system size needed for a rearrangement without any shear stress in strained periodic boundary conditions is in fact a measure of the size of the “cooperatively rearranging region” of the Adam–Gibbs theory.²

In other words, the size of the cooperatively rearranging region is the size (i.e., the box length) of the simulation cell for which shear stress vanishes for all imposed strains. By gradually increasing the system size N at constant temperature and density, computing the averaged elements of the traceless stress tensor for a number of strains at each system size, and plotting the maximum value of unrelaxed shear stress as a function of box length, one can in principle estimate the critical box length where shear stress becomes zero for all strains for a given state point. Although this is a lengthy and tedious computation that requires long simulation times (especially at high densities and low temperatures where the size would be large), there is now a definition of a correlation length that can be computed in simulations. We are currently using this method to calculate the temperature and pressure/density dependence of the correlation length in simple liquids and binary mixtures.

The results in this article show that cooperative effects in stress relaxation causing the increase of relaxation time and viscosity do not require the existence of domains of different order, although distinct domains might still appear upon supercooling and enhance the effect.

The effect is completely configurational and the same averages of the stress tensor elements would be found in a Monte Carlo simulation with strained periodic boundary conditions and minimum image convention. Similar results have in fact been obtained in Monte Carlo simulations of strained confined films, showing finite shear stress.²⁰ However, in Ref. 20 the results are enhanced by the rigid restriction of volume and rigid constraints on the boundary distribution of atoms.

ACKNOWLEDGMENTS

The author wishes to thank the National Facility of Australian Partnership for Advanced Computing for a substantial allocation of computer time for this project.

¹M. Goldstein, J. Phys. Chem. **51**, 3728 (1969).

²G. Adam and J. H. Gibbs, J. Phys. Chem. **43**, 139 (1965).

- ³P. J. Steinhardt, D. R. Nelson, and M. Ronchetti, *Phys. Rev. Lett.* **47**, 1297 (1981).
- ⁴H. Jonsson and H. C. Andersen, *Phys. Rev. Lett.* **60**, 2295 (1988).
- ⁵R. M. Ernst, S. M. Nagel, and G. S. Grest, *Phys. Rev. B* **43**, 8070 (1991).
- ⁶R. D. Mountain, *J. Chem. Phys.* **102**, 5408 (1995).
- ⁷J. P. Hansen and L. Verlet, *Phys. Rev.* **184**, 151 (1969).
- ⁸R. Agrawal and D. A. Kofke, *Mol. Phys.* **85**, 43 (1995).
- ⁹M. P. Allen and D. J. Tildesley, *Computer Simulation of Liquids* (Clarendon, Oxford, 1987).
- ¹⁰A. W. Lees and S. F. Edwards, *J. Phys. C* **5**, 1921 (1975).
- ¹¹D. J. Evans and G. P. Morriss, *Statistical Mechanics of Non-Equilibrium Liquids* (Academic, London, 1990).
- ¹²D. R. Wheeler, N. G. Fuller, and R. L. Rowley, *Mol. Phys.* **92**, 55 (1997).
- ¹³J. Delhommelle, J. Petracic, and D. J. Evans, *Phys. Rev. E* **68**, 031201 (2003).
- ¹⁴P. J. Daivis and D. J. Evans, *J. Chem. Phys.* **100**, 541 (1993).
- ¹⁵J. D. Weeks, D. Chandler, and H. C. Andersen, *J. Chem. Phys.* **54**, 5237 (1971).
- ¹⁶R. J. Speedy, *J. Chem. Phys.* **114**, 9069 (2001).
- ¹⁷M. P. Tosi and F. G. Fumi, *J. Phys. Chem. Solids* **25**, 31 (1964).
- ¹⁸J. Anwar, D. Frenkel, and M. G. Moro, *J. Chem. Phys.* **118**, 728 (2003).
- ¹⁹J. D. Honeycutt and H. C. Andersen, *Chem. Phys. Lett.* **108**, 535 (1984).
- ²⁰P. Bordarier, M. Schoen, and A. H. Fuchs, *Phys. Rev. E* **57**, 1621 (1998).